J. Shanghai Jiao Tong Univ. (Sci.), 2019, 24(5): 616-621
https://doi.org/10.1007/s12204-019-2108-0

# Low Speed Bearing Fault Diagnosis Based on EMD-CIIT Histogram Entropy and KFCM Clustering

*ZHANG Ke* (张　珂), *LIN Tianran** (林天然), *JIN Xia* (金　霞)
(School of Mechanical and Automotive Engineering, Qingdao University of Technology, Qingdao 266520, Shandong, China)



**Abstract:** In view of weak defect signals and large acoustic emission (AE) data in low speed bearing condition monitoring, we propose a bearing fault diagnosis technique based on a combination of empirical mode decomposition (EMD), clear iterative interval threshold (CIIT) and the kernel-based fuzzy c-means (KFCM) eigenvalue extraction. In this technique, we use EMD-CIIT and EMD to complete the noise removal and to extract the intrinsic mode functions (IMFs). Then we select the first three IMFs and calculate their histogram entropies as the main fault features. These features are used for bearing fault classification using KFCM technique. The result shows that the combined EMD-CIIT and KFCM algorithm can accurately identify various bearing faults based on AE signals acquired from a low speed bearing test rig.
**Key words:** empirical mode decomposition - clear iterative interval threshold (EMD-CIIT), kernel-based fuzzy c-means (KFCM), acoustic emission (AE) signals, low speed machine, roller element bearing
**CLC number:** TH 165　　**Document code:** A

## 0 Introduction

Bearings operated at a speed less than 600 r/min are referred to as low speed bearings[1]. The vibration signal generated by an incipient defect bearing operated at low speed is usually weak and quite often contaminated by a strong background noise. As a result, the impulse generated by an initial bearing defect operated at low speed is difficult to detect using the classical vibration technique. To overcome this issue, acoustic emission (AE) technique has been developed recently as an alternative technique for low speed bearing monitoring. AE has been proven to be an effective signal detection technique for low speed bearing condition monitoring (CM)[2-4]. A major advantage of AE technique is that it is not affected by the mechanical operating noise as well as the ambient noise due to the high frequency nature of the technique[5]. It can thus be employed to acquire useful bearing signals in low speed applications for accurate bearing fault diagnosis even in the presence of a strong ambient noise.

Signal processing, feature extraction and fault identification are the three major steps in low speed bearing fault diagnosis. Because AE signals generated by a defect typically have transient, non-stationary and nonlinear characteristics, signal processing techniques capable of dealing with non-stationary, nonlinear signal characteristics are needed in the analysis of AE signals. Commonly employed non-stationary signal processing techniques include wavelet transform (WT), wavelet packet decomposition (WPD), Wigner-Ville distribution (WVD), empirical mode decomposition (EMD), ensemble empirical mode decomposition (EEMD) and EMD - clear iterative interval threshold (EMD-CIIT). WT or WPD can be employed for multi-scale signal analysis by stretching and translation operation to extract useful eigenvalues of non-stationary signals in both time and frequency domains[6]. Though, deficiencies of WT technique have also been observed. For instance, Feng et al.[7] pointed out that WT technique has some inherited deficiencies such as how to select a proper mother wavelet and the overlapping of wavelet bases. EMD is another popular non-stationary signal analysis technique for bearing fault diagnosis. It is an adaptive technique suitable for decomposing non-stationary signals from which the so-called intrinsic mode functions (IMFs) are extracted from a signal to highlight the local characteristics of the signal[8]. Comparing with EMD, EEMD can effectively alleviate the mode aliasing problem of EMD[9], though it suffers from computational complexity.

A major obstacle for AE applications in low speed bearing CM is the large data volume generated during the application which poses a challenge in data storage

**Received date:** 2018-07-20
**Foundation item:** the Privileged Shandong Provincial Government's "Taishan Scholar" Program
***E-mail:** trlin@qut.edu.cn

and data processing. Lin et al.[10] proposed a down sample technique to resolve the large data issue of using AE technique. Moreover, a weak defect AE signal produced by an initial bearing defect of a low speed machine also poses a problem in the data analysis. To overcome this problem, a combined EMD-CIIT technique is utilized to enhance the strength of the defective component in an AE signal. It has demonstrated that EMD-CIIT can remove most of the noise in a signal with a small computational expense[11].

Various entropies such as energy entropy, information entropy, approximate entropy, sample entropy and histogram entropy are often employed to construct the feature vector of a signal[12-16]. For instance, the first four entropies were successfully applied in various fields, though the cumbersome iterative process in calculating these entropies poses a problem when a large amount of CM data need to be processed. Taking this into consideration, histogram entropy developed originally for image retrieval[16] is adopted in this study to extract the fault features (i.e. eigenvalues) from the AE data for low speed bearing fault diagnosis.

Once the eigenvalues are extracted from the AE signals, the next step in the proposed fault diagnosis algorithm is to identify the fault patterns from the extracted eigenvalues using machine learning techniques. Kernel-based fuzzy c-means (KFCM)[17] technique is a kernel learning based technique which can be employed for bearing fault classification. By mapping the eigenvalues into higher dimensional feature spaces, the technique can highlight and amplify the difference among the fault features, so that various fault patterns can be separated easily.

This study makes the full use of the advantage of AE technique in detecting weak bearing defect signals of a low speed machine operating in a noisy environment, and proposes a signal processing and fault diagnosis algorithm based on EMD-CIIT histogram entropy and KFCM clustering. In this algorithm, a combined EMD-CIIT is employed for noise removal and to extract the IMFs from the raw AE data. Histogram entropies are then calculated from the first three IMFs and classified using KFCM technique. The proposed algorithm is validated using a set of experimental data acquired from a low speed machine test rig. It is found that the proposed algorithm can achieve a rather high accuracy rate in the diagnosis process.

# 1 A Brief Introduction of EMD-CIIT and KFCM Clustering Algorithm

## 1.1 Clear Iterative Interval-Thresholding

Traditionally, EMD-based denoising technique is to decompose a signal into various IMF components and then calculate the correlation coefficients of the IMFs with the original signal. The IMFs having the largest correlation coefficients with the original signal are retained and the IMFs having smaller coefficients are considered as noise and are discarded[18]. Such denoising process may lead to the loss of useful components. To resolve this shortcoming, Kopsinis and Mclaughlin[19] proposed an EMD interval threshold (EMD-IT) denoising method by comparing the extreme value in the data interval defined by two subsequent zero-value data points and the threshold value. When the extreme value is larger than the threshold, all data within the interval will be preserved, otherwise the data will be discarded. It is worth noting that EMD-IT technique can also lead to data losses during the process. EMD-CIIT technique[11] has been developed to further improve the denoising effect of EMD-IT method which is employed in this study to remove the noise of the CM data. It is shown in the subsequent analysis that EMD-CIIT technique can effectively reduce the pseudo-Gibbs effect encountered in the EMD-IT denoising process.

## 1.2 Weight Factor

The principle of EMD-CIIT technique for noise removal is to use a weight factor to multiply the data so that the data are above the threshold and the data variation is amplified. In this study, we propose a data dependent weight factor ($w(n)$) to obtain a smooth noise cancellation signal in the EMD-CIIT process:

$$w(n)=\begin{cases}0, & |x_m^{\text{ext}}|\leqslant T\\ \dfrac{1}{2}-\dfrac{1}{2}\cos\left[\dfrac{\pi}{2T}(|x_m(n)|-T)\right], & T\leqslant|x_m^{\text{ext}}|\leqslant 3T,\\ 1, & |x_m^{\text{ext}}|>3T\end{cases}\quad(1)$$

where, $x_m(n)$ is the value of the $n$-th data point of the $m$-th IMF component; $x_m^{\text{ext}}$ is the extreme value of the data interval between two neighboring zero-value data points; the threshold value $T$ of the data is calculated by $T=\sigma\sqrt{2\ln N}$, $\sigma$ is the standard deviation of the data and $N$ is the data length. The standard deviation of the signal is estimated using a robust estimator on the first IMF component (IMF1):

$$\sigma_1=\frac{\text{Median}(|\text{IMF1}(n)|)}{0.674\,5},\quad n=1,2,\cdots,N.\quad(2)$$

The standard deviations of the other IMFs are

$$\sigma_m=\sqrt{\sigma_1^2/(\rho^m\beta)},\quad m=2,3,\cdots,M,\quad(3)$$

where, $\sigma_m$ is the standard deviation value of the $m$-th IMF component; $\beta$ and $\rho$ are the parameters estimated by a large number of independent noise realizations and their IMFs, 0.719 and 2.01 are the suggested values for

these two parameters[20]; $M$ is the highest order IMF component in the decomposition.

Under such approach, the data smaller than the threshold value will be discarded, the data larger than $T$ but smaller than $3T$ will be reduced using the non-linear weight factor given in Eq. (1), and the data substantially larger than $3T$ will be kept as they are.

Once the weight factor given by Eq. (1) is implemented, a denoised IMF component becomes

$$\overline{x}_m(n) = x_m(n)w(n). \tag{4}$$

As the data near the threshold will increase at a slower rate using the non-linear weight factor, the signal oscillation after the noise reduction will be much smoother.

### 1.3 Histogram Entropy

After denoising the signal, the next step is to extract the feature representing the characteristic of the signal. Histogram entropy of the signal is used to construct the eigenvector of the AE signal in this study. The histogram entropy is originally employed in image retrieval which is adopted analogically in this study as the characteristic feature of the AE signals is acquired from a low speed bearing.

### 1.4 Fuzzy Kernel Clustering

The characteristic features of a defective low speed bearing can be recognized by a classifier in the bearing fault diagnosis process. In this study, KFCM algorithm is employed as the classifier to identify the fault features obtained from the previous section. KFCM algorithm uses a kernel function to map the original feature space to a higher dimension feature space. If the samples are mapped directly to a higher dimension space and then clustered, it can be a problem in determining the parameters and the form of the nonlinear mapping function, as well as the feature space dimension. The use of the kernel function can effectively resolve this problem.

The clustering objective function of the KFCM algorithm is given by

$$\left.\begin{aligned} J_p &= \sum_{k=1}^{K}\sum_{i=1}^{I}\sum_{j=1}^{J} u_{ik}^p \|\phi(x_{ij}) - \overline{V}_{kj}\|^2 \\ 0 &\leqslant u_{ik} \leqslant 1 \\ \sum_{k=1}^{K} u_{ik} &= 1 \end{aligned}\right\}, \tag{5}$$

where, $\phi(x_{ij})$ is the $j$-th dimension eigenvalue of the $i$-th sample in the Gaussian kernel space; $\overline{V}_{kj}$ is the $j$-th dimension eigenvalue of the $k$-th class in the Gaussian kernel feature space; $K$ is the number of classes; $I$ is the number of samples; $J$ is the dimension of the eigenvalues; $u_{ik}$ is the membership degree of the $i$-th data sample to the $k$-th class and $u_{ik} \in [0,1]$; $p$ is the weighting index. The membership and the clustering centers can be calculated in the Gaussian kernel space:

$$u_{ik} = \frac{1}{\displaystyle\sum_{k'=1}^{K}\left(\frac{\displaystyle\sum_{j=1}^{J}\|\phi(x_{ij}) - \overline{V}_{kj}\|^2}{\displaystyle\sum_{j=1}^{J}\|\phi(x_{ij}) - \overline{V}_{k'j}\|^2}\right)^{\frac{1}{p-1}}}, \tag{6}$$

$$\overline{V}_{kj} = \sum_{i=1}^{I} u_{ik}^p \phi(x_{ij}) \Big/ \sum_{i=1}^{I} u_{ik}^p. \tag{7}$$

The category of a sample can be determined based on the membership degree $u_{ik}$ of each class $x_i$. For instance, if sample $x_i$ has the highest degree of membership for the $k$-th class, then $x_i$ belongs to the $k$-th class.

### 1.5 Hamming Approach Degree

The fault types of the low speed bearing are recognized by calculating the close degree of the test samples and the fault clustering center. The eigenvectors are composed of $d$ characteristic parameters corresponding to one pattern point on the $d$-dimensional feature space. There are clustering properties among similar points. The pattern points of different states have their own clustering domain and clustering center. "Maximum margin principle" is typically employed in the pattern recognition within a population model. It is defined that let $A_n$ and $B$ be the fuzzy sets, if there is a $n$-th element which satisfies:

$$\begin{aligned} &Y(A_n, B) = \\ &\quad \max\{Y(A_1, B), Y(A_2, B), \cdots, Y(A_N, B)\}. \end{aligned} \tag{8}$$

Then $A_n$ and $B$ are considered to be the closest and belong to the same category. This principle is termed as the maximum margin principle. Hamming approach degree is then deployed to calculate $Y(A, B)$:

$$Y(A, B) = 1 - \frac{1}{N}\sum_{n=1}^{N} |A(S_k) - B(S_k)|, \tag{9}$$

where $S_k$ is the characteristic parameter.

## 2 Bearing Fault Experiment and Diagnosis

A laboratory experiment was conducted on a low speed bearing test rig shown in Fig. 1 to examine the effectiveness of the EMD-CIIT histogram entropy and KFCM algorithm proposed in this study. A single-row roller element bearing (type ER16K) was used in the experiment. There are 9 roller elements with a diameter of 7.937 5 mm in the bearing. The mean diameter of the bearing is 38.506 4 mm, and the contact angle is 9.08°. Four types of bearing operation conditions (i.e.

healthy bearing, ball fault, inner race fault and outer race fault) were simulated in the experiment. The simulated bearing defects are shown in Fig. 2.

The shaft rotation speed was kept constant at 120 r/min during the experiment, and the sampling frequency of the AE signal was set at 1.2 MHz. The data length for each data sample is 1 s, and 30 data samples were acquired for each bearing fault type. An example of the AE time waveforms corresponding to the four bearing operation conditions is shown in Fig. 3.

From Fig. 3, it is difficult to differentiate the four bearing operation conditions directly from the AE time waveforms. The signals are then processed using the combined algorithm proposed in the study. The EMD-CIIT technique is employed first to remove the noise by decomposing a signal into IMF components. Figure 4 shows the 13 IMF components (IMF1—IMF13) and the remainder ($R$) of a signal representing the outer race fault calculated by the EMD-CIIT.

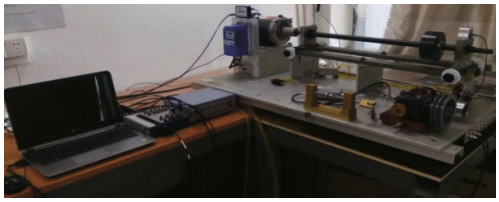

Fig. 1 The low speed bearing test rig

(a) Outer race (b) Inner race (c) Ball

Fig. 2 The simulated bearing faults in the experiment

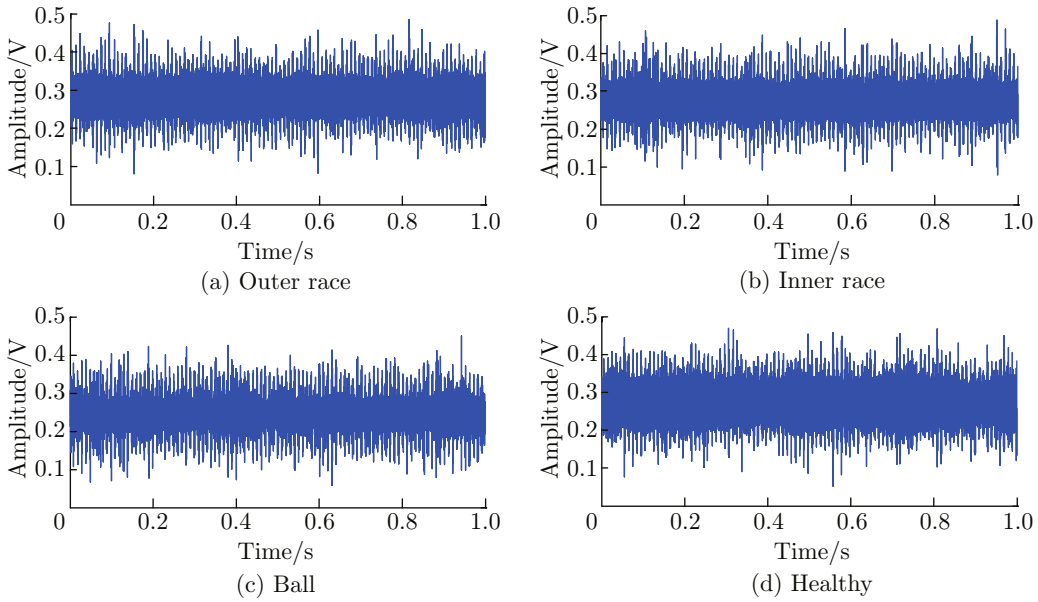


Fig. 3 The AE time waveforms corresponding to the four bearing operation conditions

The IMF components are arranged in the order from the highest to the lowest frequency components. Only the first three IMF components (IMF1—IMF3) which have the highest correlations with the original signal are retained in the process to reduce the computational cost. Histogram entropies are calculated for these three IMFs as the fault features. Four groups of feature data containing $3\times30$ histogram entropies are obtained from the first three IMFs for each of the four bearing operation conditions. 25 samples from each operation condition are used as the test samples in the clustering process, and the remaining 5 samples for each condition are used as the validation samples in the fault diagnosis process.

The clustering parameters in the recognition of eigenvalues of the data are set as follows: the number of the clustering centers is 4, the weighting index is 2, and the iteration termination tolerance is $10^{-6}$. The four groups of $3\times25$ histogram entropy data are clustered using KFCM algorithm. The calculated clustering centers from the process are listed in Table 1. The cluster center for each of the four bearing operation conditions differs from each other which implies that the histogram entropy calculated from the IMFs using the EMD-CIIT technique can be used as an effective feature for the low speed bearing fault diagnosis. The three-dimensional distribution of the eigenvalues after KFCM clustering is shown in Fig. 5. It demonstrates that the data for

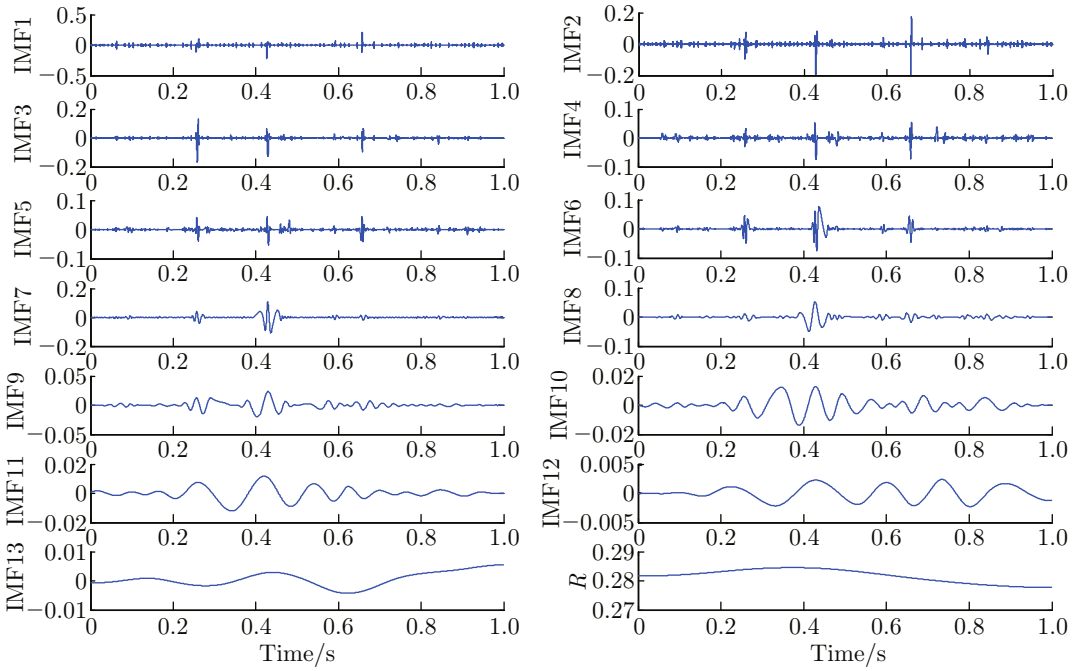


Fig. 4 Time-domain waveforms of IMFs obtained by EMD-CIIT and EMD

each of the four bearing operation conditions are clustered around the corresponding cluster center.

**Table 1 Cluster centers of EMD-CIIT + EMD + histogram entropy + KFCM**

| Cluster center | L1 | L2 | L3 |
|---|---|---|---|
| Outer race | −5.531 3 | −5.135 3 | −4.909 9 |
| Inner race | −6.069 0 | −5.794 1 | −5.644 2 |
| Ball | −4.587 0 | −4.381 5 | −4.178 9 |
| Healthy | −5.647 5 | −5.897 9 | −6.435 0 |

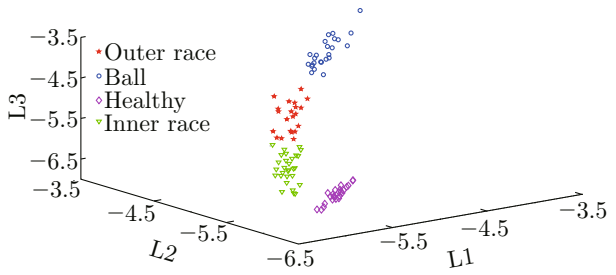


Fig. 5 Eigenvalues distributions of EMD-CIIT + EMD + histogram entropy + KFCM

After the clustering, the remaining 4 sets of $3 \times 5$ histogram entropies are used as the validating samples and calculated using the hamming approach degree to examine the reliability and effectiveness of the algorithm. The results calculated based on the maximum margin principle are listed in Table 2. It demonstrates that only two outer race fault samples are misclassified as the inner race fault. This is equivalent to an accuracy rate of 90% using the proposed algorithm.

**Table 2 Test results of EMD-CIIT + EMD + histogram entropy + KFCM**

| Sample clustering results | The close degree of the test samples and the fault clustering center | | | |
|---|---|---|---|---|
| | Outer race | Inner race | Ball | Healthy |
| 1 | 0.620 2 | 0.736 2 | −0.189 5 | 0.388 5 |
| 2 | 0.675 3 | 0.681 1 | −0.134 4 | 0.309 4 |
| 3 | 0.968 8 | 0.387 0 | 0.159 7 | 0.229 3 |
| 4 | 0.946 2 | 0.354 0 | 0.192 7 | 0.196 3 |
| 5 | 0.806 3 | 0.162 7 | 0.384 0 | 0.005 0 |
| 6 | 0.256 0 | 0.899 6 | −0.553 7 | 0.628 2 |
| 7 | 0.047 6 | 0.691 2 | −0.762 1 | 0.551 8 |
| 8 | 0.536 4 | 0.820 1 | −0.273 4 | 0.502 0 |
| 9 | 0.292 8 | 0.936 4 | −0.516 9 | 0.596 8 |
| 10 | 0.266 6 | 0.910 2 | −0.543 1 | 0.642 3 |
| 11 | 0.031 0 | −0.612 6 | 0.840 7 | −0.770 3 |
| 12 | 0.451 5 | −0.192 1 | 0.738 8 | −0.349 8 |
| 13 | 0.573 3 | −0.070 3 | 0.617 0 | −0.228 0 |
| 14 | 0.374 3 | −0.269 3 | 0.816 0 | −0.427 0 |
| 15 | 0.440 7 | −0.202 9 | 0.749 6 | −0.360 6 |
| 16 | 0.161 9 | 0.568 6 | −0.647 8 | 0.963 2 |
| 17 | 0.264 2 | 0.499 9 | −0.408 5 | 0.797 5 |
| 18 | 0.244 3 | 0.429 5 | −0.312 1 | 0.701 1 |
| 19 | 0.264 1 | 0.496 0 | −0.403 3 | 0.792 3 |
| 20 | 0.167 5 | 0.546 3 | −0.642 3 | 0.968 7 |

Note: The green font represents that the faults are correctly classified by the algorithm, and the red font represents that the faults are misclassified by the algorithm.

## 3 Conclusion

This paper presented a low speed bearing fault diagnostic technique using a combination of EMD-CIIT denoising technique and KFCM cluster algorithm. The algorithm first employed the EMD-CIIT to denoise the AE signals acquired from the low speed bearing test rig. The first three IMFs having the highest correlation with the original signal were then retained and their histogram entropies were calculated and used as the eigenvectors in KFCM clustering. Finally, the clustering center and the membership degree matrix determined from KFCM clustering and the hamming approach degree algorithm were utilized to classify the remaining dataset for bearing fault diagnosis. An accuracy of 90% is achieved by the proposed algorithm in the pattern recognition process. This implies that the classification method can be employed for the low speed bearing diagnosis and has the potential to be applied in the real life situation.

## References


[1] MBA D, RAO R B K N. Development of acoustic emission technology for condition monitoring and diagnosis of rotating machines: bearings, pumps, gearboxes, engines, and rotating structures [J]. *Shock and Vibration Digest*, 2006, **38**(1): 3-16.

[2] SMITH J D. Vibration monitoring of bearings at low speeds [J]. *Tribology International*, 1982, **15**(3): 139-144.

[3] YOSHIOKA T, FUJIWARA T. Application of acoustic emission o detection of rolling bearing failure [J]. *ASME: Production Engineering Division Publication*, 1984, **14**: 55-76.

[4] MIETTINEN J, PATANIITTY P. Acoustic emission in monitoring extremely slowly rotating rolling bearing [M]//MCINTYRE J, SLEEMAN D. Proceedings of COMADEM'99. Oxford, UK: Coxmoor Publishing, 1999: 289-297.

[5] VAN HECKE B, YOON J, HE D. Low speed bearing fault diagnosis using acoustic emission sensors [J]. *Applied Acoustics*, 2016, **105**: 35-44.

[6] PANDYA D H, UPADHYAY S H, HARSHA S P. Fault diagnosis of rolling element bearing with intrinsic mode function of acoustic emission data using APF-KNN [J]. *Expert Systems with Applications*, 2013, **40**(10): 4137-4145.

[7] FENG Z P, LIANG M, CHU F L. Recent advances in time–frequency analysis methods for machinery fault diagnosis: A review with application examples [J]. *Mechanical Systems and Signal Processing*, 2013, **38**(1): 165-205.

[8] FENG Z P, LIANG M, ZHANG Y, et al. Fault diagnosis for wind turbine planetary gearboxes via demodulation analysis based on ensemble empirical mode decomposition and energy separation [J]. *Renewable Energy*, 2012, **47**: 112-126.

[9] YU K, LIN T R, TAN J W. A bearing fault diagnosis technique based on singular values of EEMD spatial condition matrix and Gath-Geva clustering [J]. *Applied Acoustics*, 2017, **121**: 33-45.

[10] LIN T R, KIM E, TAN A C C. A practical signal processing approach for condition monitoring of low speed machinery using Peak-Hold-Down-Sample algorithm [J]. *Mechanical Systems and Signal Processing*, 2013, **36**(2): 256-270.

[11] TIAN P F, ZHANG L, CAO X J, et al. The application of EMD-CIIT lidar signal denoising method in aerosol detection [J]. *Procedia Engineering*, 2015, **102**: 1233-1237.

[12] AO H, CHENG J S, LI K L, et al. A roller bearing fault diagnosis method based on LCD energy entropy and ACROA-SVM [J]. *Shock and Vibration*, 2014, **2014**: 825825.

[13] AI Y T, GUAN J Y, FEI C W, et al. Fusion information entropy method of rolling bearing fault diagnosis based on $n$-dimensional characteristic parameter distance [J]. *Mechanical Systems and Signal Processing*, 2017, **88**: 123-136.

[14] ZHAO S F, LIANG L, XU G H, et al. Quantitative diagnosis of a spall-like fault of a rolling element bearing by empirical mode decomposition and the approximate entropy method [J]. *Mechanical Systems and Signal Processing*, 2013, **40**(1): 154-177.

[15] ZHANG L, ZHANG L, HU J F, et al. Bearing fault diagnosis using a novel classifier ensemble based on lifting wavelet packet transforms and sample entropy [J]. *Shock and Vibration*, 2016, **2016**: 4805383.

[16] ZACHARY J, IYENGAR S S, BARHEN J. Content based image retrieval and information theory: A general approach [J]. *Journal of the American Society for Information Science and Technology*, 2001, **52**(10): 840-852.

[17] TAO X M, XU J, FU Q, et al. Kernel fuzzy C-means algorithm based on distribution density and its application in fault diagnosis [J]. *Journal of Vibration and Shock*, 2009, **28**(8): 61-64 (in Chinese).

[18] LIN T R, YU K, TAN J W. Condition monitoring and fault diagnosis of roller element bearing [EB/OL]. (2017-05-31) [2018-07-20]. https://www.intechopen.com.

[19] KOPSINIS Y, MCLAUGHLIN S. Development of EMD-based denoising methods inspired by wavelet thresholding [J]. *IEEE Transactions on Signal Processing*, 2009, **57**(4): 1351-1362.

[20] FLANDRIN P, RILLING G, GONCALVES P. Empirical mode decomposition as a filter bank [J]. *IEEE Signal Processing Letters*, 2004, **11**(2): 112-114.